

Molecular BioSystems

Accepted Manuscript



This is an *Accepted Manuscript*, which has been through the Royal Society of Chemistry peer review process and has been accepted for publication.

Accepted Manuscripts are published online shortly after acceptance, before technical editing, formatting and proof reading. Using this free service, authors can make their results available to the community, in citable form, before we publish the edited article. We will replace this *Accepted Manuscript* with the edited and formatted *Advance Article* as soon as it is available.

You can find more information about *Accepted Manuscripts* in the [Information for Authors](#).

Please note that technical editing may introduce minor changes to the text and/or graphics, which may alter content. The journal's standard [Terms & Conditions](#) and the [Ethical guidelines](#) still apply. In no event shall the Royal Society of Chemistry be held responsible for any errors or omissions in this *Accepted Manuscript* or any consequences arising from the use of any information it contains.



www.rsc.org/molecularbiosystems

Quantitative Proteomic Analyses of the *Schistosoma japonicum* in Response to Artesunate

Qing-Ming Kong^a, Qun-Bo Tong^a, Di Lou^a, Jian-Zu Ding^a, Bin Zheng^a, Rui Chen^a,
Xiao Zhu^b, Xiao-Heng Chen^a, Ke-Wei Dong^a, Shao-Hong Lu^{*a},

^a Department of Immunity and Biochemistry, Institute of Parasitic Disease, Zhejiang Academy of Medical Sciences, Hangzhou, China.

^b Guangdong Province Key Laboratory of Medical Molecular Diagnosis, Guangdong Medical College, Dongguan, China

*Corresponding author

Email addresses:

QMK: qmkong_1025@163.com

QBT: tongqunbo@hotmail.com

DL: loudi70@163.com

JZD: dingjianzu@163.com

BZ: misszhengbin@163.com

RC: chenrui75@163.com

XZ: bioxzhu@yahoo.com

XHC: 874270150@qq.com

KWD: dong.kewei0@163.com

SHL: lssh2003@163.com

Keywords

Drug proteome, *Schistosoma japonicum*, Artesunate

Abstract

Artesunate (ART) has high prophylactic efficacy against *Schistosoma japonicum* infections and has been used to treat and prevent schistosomiasis in China since 1995. However, the molecular mechanism of ART's effects on *S. japonicum* remains unclear. Herein, we applied isobaric tagging reagents for relative and absolute quantification analysis coupled with two-dimensional liquid chromatography and tandem mass spectrometry to investigate the effect of ART on the proteome of *S. japonicum* in susceptible mice. 4529 proteins were quantified on the basis of 21825 unique peptides. Comparative proteomic analyses revealed that 145, 228 and 185 proteins were significantly differentially expressed after ART treatment in schistosomula, juvenile and adult worms, respectively. Ninety proteins were differentially expressed between each two treatment groups in response to ART treatment: 67 proteins were associated with *S. japonicum* development/aging and 23 were specifically associated with ART treatment. Quantitative real-time PCR of selected genes verified the proteomic data. Gene ontology annotation and Kyoto encyclopedia of genes and genomes pathway mapping analysis showed that the majority of differentially expressed proteins were involved in stress/defense/detoxification, signal transduction, carbohydrate metabolism, amino acid metabolism, transcription/translation, and protein synthesis/assembly/degradation. Thirty-four of the proteins differentially expressed under ART treatment encoded hypothetical, uncharacterized proteins with unknown functions. This study obtained the first comprehensive protein expression profile of *S. japonicum* in response to ART, and provided the basis for a better understanding of the molecular mechanisms of ART effects on *S. japonicum*.

Introduction

Human schistosomiasis, caused by trematode flukes of the genus *Schistosoma*, is one of world's most prevalent tropical diseases. By conservative estimates, at least 230 million people worldwide are infected with *Schistosoma* spp.¹. In 74 developing countries in the tropics and sub-tropics, almost 800 million people, mostly children, face risk of infection². The disease burden is estimated to exceed 70 million disability-adjusted life-years³ and leads to remarkably high rates of years lived with disability. Currently, preventive public health measures in endemic regions consist of treatment once every 1 or 2 years with praziquantel to suppress morbidity^{4,5}.

Praziquantel is effective against all schistosoma species, but has poor activity against immature schistosome larvae^{6,7}. Moreover, drug resistance has been noted: some isolates of *Schistosoma mansoni* showing resistance to high doses of praziquantel have been found in many foci⁸. Artemisinin and its derivatives, such as artemether and artesunate (ART), were developed as antimalarial drugs, but also kill immature larval forms of developing schistosomes. A randomized, double-blind placebo-controlled clinical trial of artemether in an area of western Cote d'Ivoire endemic for *S. mansoni* showed that oral artemether was safe and had a good prophylactic effect against *S. mansoni*⁹. In areas of continuous transmission, these compounds could be used in conjunction with praziquantel to improve overall cure rates and provide effective infection control¹⁰.

ART has been used to treat and prevent *S. japonicum* infections in China since 1995. Our previous research, including animal experiments and field trials, demonstrated good efficacy of ART for killing schistosomulas with few side effects¹¹. However, the effect of ART on *S. japonicum* decreased after 10 years of use in China¹². Thus, more studies to determine ART targets and drug resistance should be performed to

improve the prevention, control and elimination of this disease. Over the past 30 years, notable progress in pharmacological and molecular studies has been made to understand behaviors associated with ART and artemether treatment¹³.

Administration of artemether results in a reduction of the worm glycogen and protein content¹⁴, inhibition of enzymes involved in glycolysis^{15,16}, inhibition of ATPase activity¹⁷, and affects the worm antioxidant system^{18,19}. However, the molecular mechanism of how artemether acts on schistosomes remains unknown.

Proteomic analysis is a powerful tool to screen samples derived from pathogens and to identify proteins possibly involved in pathogenesis. Recent expansion of sequence databases for *S. mansoni* and *S. japonicum* have opened up new opportunities for proteomic analysis of schistosomes to better understand the parasite biology and host-parasite interactions^{20,21}. In this study, the proteomic expression profile of *S. japonicum* in response to ART was determined by isobaric tagging reagents for relative and absolute quantification (iTRAQ) analysis coupled with two-dimensional liquid chromatography and tandem mass spectrometry (2-DLC/MS-MS). The results of this study will help to identify molecules that perform various cellular functions such as redox homeostasis, stress response, protein synthesis and energy metabolism in response to ART. These results provide valuable information on ART's primary targets for the control of schistosomiasis.

Results

iTRAQ-based proteomics analyses of differentially expressed proteins.

Soluble proteins extracted from the collected schistosomula, juvenile and adult worms were compared by iTRAQ-based proteomics analyses. In total, 4529 proteins were quantified on the basis of 21825 unique peptides. Among these proteins, 4503

proteins had quantitative information in all samples (Table S1). One hundred and forty-five proteins were differentially expressed in the 10-day schistosomula after drug treatment. Two hundred and twenty-eight proteins were differentially expressed in the 17-day juvenile worms after drug treatment. One hundred and eighty-five proteins were differentially expressed in the 24-day adult worms after drug treatment. In addition, 19 proteins that showed a statistically significant change after drug treatment were common in worms from all three stages (Fig. 1B). Among the 90 proteins (Table S2) that showed a statistically significant change between each two developmental stages treated with ART, 22 were upregulated and 37 were downregulated in schistosomula, 59 were upregulated and 16 were downregulated in juvenile worms, 22 were upregulated and 43 were downregulated in adult worms (Fig. 1A). The expression levels of 156 proteins changed between each two developmental stages without treatment from schistosomula to adult worms (Fig. 1C). The 90 differentially expressed proteins were subsequently classified into two categories based on whether proteins with significant expression changes in response to ART depended on the age of the worm: 67 aging and drug-related proteins (ADRP) and 23 drug-related-only proteins (DROPs) were identified (Fig. 1D). The ADRPs group consisted of proteins that showed changes in expression during *S. japonicum* aging that could be retarded or antagonized by ART treatment. The DROPs group was composed of proteins that displayed changes in expression in response to the ART treatment alone. The detailed roles of ADRPs and DROPs are discussed later.

Quantitative real-time PCR analysis of proteins.

To verify experimentally the accuracy of identification of differentially expressed proteins by iTRAQ-based proteomics analysis, nine genes were chosen by stratified

cluster random sampling from different functional categories for quantitative real-time PCR (qPCR) analysis to quantify their transcript levels. Samples treated under the same conditions were used for the qPCR and iTRAQ experiments. Data from qPCR and iTRAQ of nine selected genes were compared and found to be mostly consistent, which suggested that these proteins identified as differentially expressed were regulated at the level of transcription (Fig. 2). Three genes displayed similar expression patterns to their protein levels, including the SJCHGC06635 protein, eukaryotic translation initiation factor 4 gamma, and 2-oxoglutarate dehydrogenase E2 component. The expression levels of four genes were different to their protein levels in one or two stages, including thioredoxin-like 2, carbonyl reductase 1, SJCHGC03473 protein and peptidyl-prolyl cis-trans isomerase. Two genes, Stress-induced-phosphoprotein 1, and 26 proteasome complex subunit DSS1, showed poor agreement with corresponding protein expression levels at all three stages, probably resulting from various post-translational modifications under ART stress, such as protein phosphorylation and glycosylation.

Functional classification and localization of differentially expressed proteins.

As predicted by gene ontology (Fig. 3A), the differentially expressed proteins were involved in stress/defense/detoxification (14.44%), signal transduction (15.56%), carbohydrate, amino acid and lipid metabolism (6.67%), cellular iron ion homeostasis (2.22%), protein synthesis/assembly/degradation (7.78%), regulation of gene expression (15.56%), and function unknown (37.78%). The cellular localizations (Fig. 3B) of the 90 differentially regulated proteins were: 20% in the nucleus, 13.33% in the membrane, 6.67% in the cytoplasm, 8.87% in the mitochondrion, 4.44% in the ribosome, 2.22% in the ubiquitin proteasome and lysosome, 3.33% in the extracellular region, and 41.11% unknown. Our results demonstrated that most of the identified

proteins involved in stress/defense/detoxification and signal transduction were located in the mitochondrion and the membrane.

Discussion

ART shows a high prophylactic efficacy against *S. japonicum* infections. However, no curated or predicted pathogen genes have been identified as associated with this compound (<http://tdrtargets.org/>) and the exact mechanism of how artemether acts on schistosomes remains elusive. In the current study, we used an iTRAQ-based proteomic approach to quantitatively profile *S. japonicum* proteins that responded to ART treatment. The iTRAQ-based LC-MS/MS analysis identified 4529 proteins, of which 90 were differentially expressed. To understand how the expression of these proteins changed in response to *S. japonicum* aging and ART exposure, they were divided into two categories: ADRPs (67 proteins), which showed changes in expression during *S. japonicum* aging that could be retarded or antagonized by ART treatment and DROPs (23 proteins), whose expressions did not change during the aging process but changed only in response to ART exposure. We hypothesized that the DROPs might be more important in response to ART. Of the 90 differentially expressed proteins, 34 were newly identified and were of unknown function. The functions of the remaining 56 proteins that were strongly regulated by ART, were related to stress/defense/detoxification, signal transduction, carbohydrate metabolism, amino acid metabolism, transcription/translation, and protein synthesis/assembly/degradation (Fig. 4)

We proposed the most significant pathway ($p < 0.05$) of ART stress responses in *S. japonicum* after pathway enrichment analyses (Fig. 5). The enriched pathways included drug metabolism-cytochrome P450, hematopoietic cell lineage, glutathione metabolism, and RNA degradation. In the current study, the protein SJCHGC09008

involved in xenobiotics metabolism by cytochrome P450 showed a statistically significant change between the first two ART-treated developmental stages. The cytochrome oxidase of *Plasmodium berghei* was also inhibited completely by sodium artesunate²². The SJCHGC06865 protein is a porphyrin metabolism-related protein that also showed a statistically significant change between each two ART-treated developmental stages. One of the best-known porphyrins is heme, and heme detoxification is crucial in artemisinin's action against malaria. Heme-artemisinin adducts are crucial mediators of the ability of artemisinin to inhibit heme polymerization, which results the death of the malaria parasite²³. Glutathione metabolism-related proteins play vital roles in antioxidant pathways and are considered potential drug targets for the development of antischistosomal chemotherapy²⁴. Proteins SJCHGC06612 and SJCHGC05326 are two glutathione metabolism-related proteins that showed a statistically significant change between each two ART-treated developmental stages. A number of studies have demonstrated that hematin within the reducing environment, such as cysteine protease, aspartic proteases plasmepsin I and plasmepsin II, would produce a pool of heme capable of activating ART²⁵⁻²⁷. In the present work, the expression level of cysteine protease related protein showed a statistically significant change after ART treatment. The activated ART form adducts with a variety of biological macromolecules can clear *Plasmodium falciparum* infections rapidly by the inhibition of the sarco/endoplasmic reticulum calcium-dependent ATPase²⁸. The calcium-dependent activator protein for secretion (CAPS) also showed a statistically significant change after ART treatment with developmental stages in current study.

Some stress/defense/detoxification-related proteins were identified as responding to ART. Carbonyl reductase is a member of a significant pathway for the detoxification of reactive aldehydes derived from lipid peroxidation, drug metabolism and resistance

²⁹. Carbonyl reductase 1 (CBR1) showed a statistically significant change between each two ART-treated developmental stages in the current study. Stress-induced-phosphoprotein (Hop) is one of the best-studied co-chaperones of the Hsp70/Hsp90 complex. Upregulation of stress-induced-phosphoprotein 1 in the current study indicated that stress-induced-phosphoprotein 1 could be an excellent *S. japonicum* drug target, as it is in malaria ³⁰. Leucine zipper-EF-hand containing transmembrane protein 1 (LETM1) is a component of the Ca²⁺/H⁺ antiporter ³¹. LETM1 has a distinct role in the maintenance of mitochondrial volume and shape, which, in concert with AAA-ATPase BCS1L, achieves the efficient assembly of the respiratory chains³². Upregulation of LETM1 and AAA-ATPase in the current study might function to maintain mitochondrial biogenesis in the drug stress environment. Copper is an essential element for life via its involvement in free-radical detoxification, mitochondrial oxidative phosphorylation, neurotransmitter synthesis and iron metabolism; however, excessive copper can be toxic or even lethal to the cell ³³. The expression level of solute carrier family 31, member 1 (SLC31A1), a copper transporter, decreased after ART treatment during development in the current study, which suggested that SLC31A1 might play a crucial role in maintaining a critical copper balance or buffering of strict copper regulation. Mitochondrial carrier protein-related (G4LZA6) belongs to the mitochondrial carrier (MC) family, which are involved in transporting keto acids, amino acids, nucleotides, inorganic ions and co-factors across the mitochondrial inner membrane. One of the MC family members, the uncoupling protein, an long-chain fatty acids anion/H⁺ symporter, functions to transporting fatty acids, long chain alkylsulfonates and chloride ³⁴. A similar long-chain fatty acids -dependent mechanism of transmembrane H⁺ transport may involve mitochondrial carrier protein-related (G4LZA6) and be responsible for mitochondrial uncoupling and regulation of metabolic efficiency in response to ART. TRIM56 is an

interferon-inducible E3 ubiquitin ligase that modulates stimulator of interferon genes (STING) to confer double-stranded DNA-mediated innate immune responses³⁵.

Downregulation of TRIM56 proteins after ART treatment during development might result in reduced resistance of the immune system to ART, resulting in the eventual death of worm cells.

At present, little is known about signal transduction mechanisms in schistosomes. In the present work, Aquaporin-3 (AQP-3), Discoidin domain receptor (DDR), Sh3 domain protein, protein kinase, protein kinase B (PKB), calcium-dependent activator protein for secretion (CAPS), serine/threonine protein phosphatase 1 regulatory subunit 10, protein phosphatase inhibitor-2 (IPP-2), Leucine-rich repeat (LRR) domain protein, G protein, β -arrestin 1, and Notchless protein homolog 1 (Nle1) showed significant changes in expression under ART treatment. These proteins are involved in the signal transduction belonging to biological regulation, cell adhesion, glutamatergic synapse, endocytosis and exocytosis, water reabsorption, and the notch signaling pathway. Administration of artemether results in damage to the tegument and musculature of schistosomula. AQP is the most abundant transmembrane protein in the tegument of the schistosome. AQP expression increased after ART treatment with developmental stages in the current study and seems to be essential to parasite survival, related to the crucial role in osmoregulation, nutrient transport and drug uptake³⁶. DDRs are receptor tyrosine kinases (RTKs) that recognize collagens as their ligands. These intriguing and unique receptors play important biological roles in cell adhesion, cell growth, differentiation and metabolism^{37,38}. Phosphorylation of tyrosine residues within the intracellular domains of activated DDRs generates docking sites for Sh2, Sh3, and PTB domain-containing proteins^{39,40}. These protein complexes, as in all RTKs, result in the activation of distinct DDR-initiated signaling pathways. Serine/threonine kinase, also

known as PKB, can be activated by RTKs, G-protein coupled receptors (GPCRs), and other stimuli thus mediating many of downstream events, including cell proliferation, glucose metabolism and many synthetic and secretory pathways⁴¹⁻⁴³. The CAPS also increased after ART treatment with developmental stages in current study. This family consists of two members (CAPS1 and CAPS2) that regulate exocytosis of catecholamine-containing or neuropeptide-containing dense-core vesicles at secretion sites such as nerve terminals⁴⁴. PKB, with regions that associate with protein phosphatase-1 (PP1) and IPP-2, can form a regulatory complex to differentially regulate glycogen synthase kinase-3 (GSK3) dephosphorylation^{45,46}. GTP-binding proteins (G proteins) are membrane-associated, heterotrimeric proteins composed of three subunits: alpha, beta, and gamma. LRR containing GPCRs belong to the large GPCRs superfamily but are unique in having a large ectodomain important for ligand binding. LRR, a protein structural motif with α/β horseshoe fold⁴⁷, is frequently involved in the formation of protein-protein interactions⁴⁸. G proteins and GPCRs form one of the most prevalent signaling systems, regulating events as diverse as cell growth and cellular homeostasis^{49,50}. GPCRs are critically regulated by β -arrestins, which not only desensitize G-protein signaling but also initiate a G-protein-independent wave of signaling⁵¹. β -arrestin has a major role in Notch signaling as a regulator⁵². The notch signaling pathway functions as a critical controller of cell fate decisions and is a key regulator of cell growth, differentiation, and proliferation. Notchless (Nle), mutant alleles of Notch, is a modulator that maintains Notch activity levels in balance⁵³. The death of mouse Nle-deficient embryos might result from abnormal Notch signaling during the first steps of development⁵⁴. Nle1 also has similar functions during embryonic development in mammals⁵⁵. Changes in the expressions of AQP-3, DDR, Sh3 domain protein, protein kinase, PKB, CAPS, serine/threonine protein phosphatase 1 regulatory subunit 10, IPP-2, LRR domain

protein, G protein, β -arrestin 1, and Nle1 in response to ART would help *S. japonicum* to resist or adapt to drug stress. These proteins may represent viable targets for chemotherapeutic or immunological intervention.

Administration of ART or artemether results in reduction of worm glycogen and protein content, inhibition of phosphoglycerate kinase (PGK), pyruvate kinase (PK), phosphoglycerate mutase (PGM), and enolase (ENO)-related enzymes involved in glycolysis^{6, 7, 56}. Our results showed that six (6.67%) proteins involved in metabolism were differentially expressed, of which two are involved in glycolysis, one in the tricarboxylic acid (TCA) cycle, two in amino acid metabolism and one in lipid metabolism. Glycogen synthase kinase-3 (GSK-3) was discovered in the context of its involvement in regulating glycogen synthase, which is regulated by a complex comprising PKB with regions that associate with protein phosphatase-1 and protein phosphatase inhibitor-2^{45, 46}. Downregulation of GSK-3 in the current study is consistent with the previously reported reduction in worm glycogen levels.

The majority of proteins identified in previous studies, such as the sarco/endoplasmic reticulum calcium-dependent ATPase (PfATP6), heme and translational controlled tumor protein (TCTP)²⁸, have significant effects in response to malaria treatment with artemisinin. In the present study, these proteins remained unchanged suggesting that ART may have a different mechanism of action on *S. japonicum*. Of the 90 differentially expressed proteins under ART pressure, 34 proteins (37.78%) were newly identified as hypothetical, uncharacterized proteins with unknown functions. Among these new identified proteins, nine proteins were strongly regulated by ART during development, of which five belonged to DROPs and four to ADRPs. Their accession numbers in the UniProt database are C1LGT8, Q5DF01, Q5BXEO, Q5DGF9, Q5BWX4; and Q5D8G7, G4VGL8, G4V9Q7, C4QM44, respectively.

Further studies on the functions of these new proteins may provide a basis for a better

understanding of the molecular mechanisms of ART's effects on *S. japonicum* infection.

Our results showed that iTRAQ is a powerful technique for quantitative proteome analysis of *S. japonicum* in response to the sesquiterpene lactone compound ART. Ninety differentially expressed proteins that responded to drug stress, including 34 function unknown proteins, were identified. The known proteins were mainly involved in stress/defense/detoxification, signal transduction, carbohydrate metabolism, amino acid metabolism, cellular iron ion homeostasis, transcription/translation, and protein synthesis/assembly/degradation. Down regulation or inhibition of protein expression may be required for worm survival and growth under drug stress, and may help them to adjust to oxidative stress. In contrast, protein up regulation indicated that antioxidative reactions were occurring. In summary, the present study: 1) established a comprehensive proteomic index of *S. japonicum* in response to the sesquiterpene lactone compound ART; and 2) increased our understanding of molecular processes involved in regulatory networks responding to drug stress. To identify the direct binding targets of ART, the downstream effector molecules of the subsequent damage the drug causes and to clearly determine the mode of action of this drug, the biological function of proteins that significantly changed after drug administration must be further studied.

Experimental

Ethics statement.

All procedures carried out on animals within this study were conducted following the guidelines of the Association for Assessment and Accreditation of Laboratory Animal Care International (License number 001489). The Institutional Animal Care and Use

Committee (IACUC) of the Zhejiang Academy of Medical sciences approved the animal study protocol with the Ethical Clearance Number ZJAMS20140012.

Drug Treatment and Worm Collection.

Imprinting Control Region mice (body weight, 20 g each) and New Zealand rabbits (body weight, 2000 g each) were purchased from the Zhejiang Provincial Experimental Animal Center, China (Hangzhou). They were raised in a sterilized room and fed sterilized food and water. The *S. japonicum* (Anhui isolate) life forms were maintained in *Oncomelania hupensis* snails and New Zealand rabbits. Cercariae were collected by exposing infected snails to light to induce shedding. Cercarial numbers and viability were determined by direct observation under a light microscope. Imprinting control region mice were infected with 200 cercariae each and were orally administered with ART (the ART group) in 1% sodium carboxymethylcellulose (CMC) at a dose of 120 mg/kg at 7, 14, and 21 days post infection (dpi). As the control (CON) group, mice were administered with 1% CMC only. Worms were obtained by perfusion of infected mice at 10 dpi (group 1, schistosomula), 17 dpi (group 2, juvenile worms), and 24 dpi (group 3, adult worms), respectively. The worms were manually washed in phosphate buffered saline at 37 °C to remove any residual host proteins. The collected worms from the three groups were designated as CON1, ART1, CON2, ART2, CON3, and ART3, respectively, and were snap frozen and stored in liquid nitrogen until use.

Protein Preparation and Labeling with iTRAQ Reagents.

Lysis buffer (8 M urea, 40 mM HEPES pH = 7.4) supplemented with protease inhibitor (Roche Applied Science, Mannheim, Germany) was added to the frozen samples, which were then homogenized carefully. The mixture was sonicated for 5

min (pulse durations of 10 s on and 15 s off) in an ice bath sonicator. The unlysed worms and debris were removed by centrifugation at $15000 \times g$ at 4°C for 10 min. Supernatants containing worm proteins were transferred into new tubes and purified using the 2D Clean-Up Kit (GE healthcare, Fairfield, CT, USA), according to the manufacturer's instructions, to remove contaminating materials. All samples were quantified using a RC-DC Protein Assay Kit (Bio-Rad, Hercules, CA, USA) and aliquots were stored at -80°C .

Protein digestion was performed according to the filter-aided sample preparation procedure described by Wisniewski⁵⁷. The resulting peptide mixture was labeled using the 8-plex iTRAQ reagent (AB SCIEX, Framingham, MA, USA), according to the manufacturer's instructions. Briefly, 200 μg of proteins from each sample were incorporated into 30 μL STD buffer (4% SDS, 100 mM DTT, 150 mM Tris-HCl, pH 8.0). The detergent, DTT and other low-molecular-weight components were removed using UA buffer (8 M Urea, 150 mM Tris-HCl, pH 8.0) and repeated ultrafiltration (Microcon units, 30 kDa). 100 μL of 0.05 M iodoacetamide in UA buffer was then added to block reduced cysteine residues and the samples were incubated for 20 min in the dark. The filters were washed with 100 μL UA buffer three times and then with 100 μL DS buffer (50 mM triethylammoniumbicarbonate at pH 8.5) twice. Finally, the protein suspensions were digested with 2 μg sequencing-grade trypsin (Promega, Madison, WI, USA) in 40 μL DS buffer at 37°C for 16 h. The protein digests were estimated by UV light spectral density at 280 nm using an extinction coefficient of 1.1 of 0.1% (g/L) solution, which was calculated on the basis of the frequency of tryptophan and tyrosine in vertebrate proteins. The protein digests were desalted using Sep-Pak C18 cartridges (Waters, Milford, MA, USA) and dried in a speedvac (Thermo Electron, Waltham, MA, USA). For labeling, desalted samples were reconstituted in 70 μL of dissolution buffer and mixed with different iTRAQ reagents.

Peptides from samples CON1, CON2, CON3, ART1, ART2 and ART3 were labeled with iTRAQ reagent 113, 114, 115, 116, 117, and 119, respectively. One sixth of the six sample digests above were pooled together as an internal standard and labeled with iTRAQ reagent 121. The iTRAQ labeled treatment and control sample digests were combined into one sample mixture and dried using a speedvac for strong cation exchange fractionation.

Strong Cation Exchange (SCE) Fractionation of Peptide Mixtures.

iTRAQ labeled peptides were fractionated by SCX chromatography using the AKTA purifier system (GE Healthcare, Fairfield, CT, USA). The dried peptide mixture was reconstituted and acidified with 2 ml of buffer A (10 mM KH_2PO_4 in 25% of ACN, pH 2.7) and subjected to a Polysulfoethyl A column (100 mm \times 4.6 mm, 200-Å pore size, 5 μm particle size) (PolyLC, Columbia, MD, USA) on a Waters Delta 600 HPLC unit (Waters, Milford, MA, USA). The peptides were eluted at a flow rate of 1 ml/min with a gradient of 0%–10% buffer B (500 mM KCl, 10 mM KH_2PO_4 in 25% of ACN, pH 2.7) for 2 min, 10–20% buffer B for 25 min, 20%–45% buffer B for 5 min, and 50%–100% buffer B for 5 min. Elution was monitored by absorbance at 214 nm, and fractions were collected every 1 min. The collected fractions (about 30 fractions) were combined into 10 pools and desalted on C18 Cartridges (Sigma-Aldrich Chemical Co, St. Louis, MO, USA). Each fraction was concentrated by vacuum centrifugation and reconstituted in 40 μL of 0.1% (v/v) trifluoroacetic acid. Samples were stored at -80°C before MS experiments.

LC-MS/MS Analysis.

LC-MS/MS experiments were performed on a Q Exactive mass spectrometer coupled to an Easy nLC (Thermo Fisher Scientific Inc, San Jose, CA, USA). 10 μL of each

fraction was injected for nanoLC-MS/MS analysis. The peptide mixture (5 µg) was loaded onto a C18-reversed phase column (Thermo Scientific Easy Column, 10 cm long, 75 µm inner diameter, 3 µm resin) in buffer A (0.1% Formic acid) and separated using a linear gradient of buffer B (80% acetonitrile and 0.1% Formic acid) at a flow rate of 250 nl/min controlled by IntelliFlow technology over 140 min. MS data was acquired using a data-dependent top10 method, choosing dynamically the most abundant precursor ions from the survey scan (300–1800 m/z) for higher-energy collisional dissociation fragmentation. Determination of the target value was based on predictive automatic gain control. The dynamic exclusion duration was 60 s. Survey scans were acquired at a resolution of 70,000 at m/z 200 and the resolution for higher-energy collisional dissociation spectra was set to 17,500 at m/z 200. The normalized collision energy was 30 eV and the underfill ratio, which specifies the minimum percentage of the target value likely to be reached at maximum fill time, was defined as 0.1%. The instrument was run with the peptide recognition mode enabled.

Protein Identification and Quantification.

MS data were acquired using data-dependent acquisition conditions. The instrument was operated in the positive ion mode, and each MS event was followed by MS2 scans on the top eight most intense peaks; the MS2 activation type was pulsed Q collision-induced dissociation. Pulsed Q collision-induced dissociation parameters were set at an isolation width of 2 m/z, normalized collision energy of 35%, an activation Q of 0.7, and activation time of 0.1 ms, based on Griffin et al.⁵⁸. The threshold for MS/MS acquisition was set to 500 counts. MS/MS spectra were searched using the MASCOT engine (Matrix Science, London, UK; version 2.2) embedded into Proteome Discoverer 1.3 (Thermo Fisher Scientific Inc, San Jose, CA, USA) against Uniprot Schistosoma database (29356 sequences, download at January

23rd, 2014) and the decoy database. For protein identification, the following options were used. Peptide mass tolerance = 20 ppm, MS/MS tolerance = 0.1 Da, Enzyme = Trypsin, Missed cleavage = 2, Fixed modification: Carbamidomethyl (C), iTRAQ8plex (K), iTRAQ8plex (N-term), Variable modification: Oxidation (M), FDR ≤ 0.01 ⁵⁹. Unlabeled peptides and those containing decoy sequences were removed. Summed intensity normalization was then performed to ensure that each iTRAQ reporter had the same total intensity.

Statistical Analyses and Bioinformatic Analyses

Statistically significant changes were weighted by the error factor (a measure of the variation between the different iTRAQ ratios for the reagent pair) and p value⁶⁰. A protein a fold change of > 1.20 or < 0.83 and with a corrected p value < 0.05 was considered significantly differentially expressed. Functional protein analyses were extracted using the AmiGO tool in the gene ontology platform (<http://www.geneontology.org/>). Pathway analyses were extracted using the Search pathway tool in the Kegg Mapper platform (<http://www.genome.jp/kegg/mapper.html>). The pathway enrichment statistics was performed by Fisher's Exact Test, and with a corrected p value < 0.05 was considered the most significant pathways.

Quantitative Real-time PCR Verification.

RNA was extracted using the TRIZOL Reagent (Thermo Fisher Scientific Inc, San Jose, CA, USA) and genomic DNA was removed by digesting each sample with DNaseI (Promega, Madison, WI, USA). The samples were quantified spectrophotometrically using a Biophotometer (Eppendorf, Barkhausenweg, Hamburg, Germany). Six micrograms of purified worm mRNA obtained by perfusion of

infected mice, the same as in MS, were used as the template for reverse transcription (RT) reaction performed with random hexamer primers and Superscript III reverse transcriptase (Thermo Fisher Scientific Inc, San Jose, CA, USA), according to standard protocols. The resulting cDNAs were used for quantitative PCR.

Quantitative real time PCR was conducted on triplicate samples using SYBR Green tag in a 7500 Fast Real-Time PCR System (Thermo Fisher Scientific Inc, San Jose, CA, USA). Gene-specific primers were designed using Primer 5.0 (Table S3). The TPC2L and NADH dehydrogenase genes were used as references for normalization⁶¹.⁶² Reaction conditions and cycling protocols were followed as described in the SYBR green tag kit to add the fluorescent tag during every final extension step. Negative (no template) controls were included in each PCR run. Quantitation of relative differences in expression was calculated using the Applied Biosystems 7500 system Software v2.0.6.

Role of personnel

Conceived and designed the experiments: LSH, KQM, and CR.

Performed the experiments: KQM, LD, TQB, DJZ, ZB, ZX, CXH, DKW, and CR.

Analyzed the data: KQM, ZX.

Contributed reagents/materials/analysis tools: KQM, ZX, LD, TQB, DJZ, ZB, and CXH.

Contributed to the writing of the manuscript: KQM, LSH, and CR.

Acknowledgements

This work was supported by the Zhejiang Provincial Natural Science Foundation of China (Y2110957), International S&T Cooperation Program of China (2013DFG32960), Science and Technology Planning Project of Zhejiang Province, China (2012C33014), the Projects of Zhejiang Health Department (XKQ-009-003, XKQ-010-001), the PhD Start-up Fund of Zhejiang Academy Medical Sciences and

Zhejiang provincial Program for the Cultivation of High level Innovative Health Talents. The funders had no role in study design, data collection and analysis, decision to publish, or preparation of the manuscript. We greatly acknowledge the study participants and their families. We thank Shanghai Applied Protein Technology Co., Ltd for help in protein analysis and XG Zhang, YR Liu and JN Liu from LC-Bio for iTRAQ data analysis. We would like to thank the native English speaking scientist of Elixigen Company for editing our manuscript.

References

1. Colley DG, Bustinduy AL, Secor WE, King CH, *Lancet*, 2014, **383**, 2253-64
2. King CH, *Acta Trop*, 2010, **113**, 95-104
3. Gray DJ, McManus DP, Li Y, Williams GM, Bergquist R, Ross AG, *Lancet Infect Dis*, 2010, **10**, 733-6
4. Doenhoff MJ, Pica-Mattoccia L, *Expert Rev Anti Infect Ther*, 2006, **4**, 199-210
5. Wu W, Huang Y, *Parasitol Res*, 2013, **112**, 909-15
6. Xiao SH, Keiser J, Chen MG, Tanner M, Utzinger J, *Adv Parasitol*, 2010, **73**, 231-95
7. Xiao SH, *Acta Trop*, 2005, **96**, 153-67
8. Wang W, Wang L, Liang YS, *Parasitol Res*, 2012, **111**, 1871-7
9. Utzinger J, N'Goran EK, N'Dri A, Lengeler C, Xiao S, Tanner M, *Lancet*, 2000, **355**, 1320-5
10. Utzinger J, Keiser J, Shuhua X, Tanner M, Singer BH, *Antimicrob Agents Chemother*, 2003, **47**, 1487-95
11. Li S, Wu L, Liu Z, Hu L, Xu P, Xuan Y, Liu Y, Liu X, Fan J, *Chin Med J (Engl)*, 1996, **109**, 848-53
12. Hua HY, Liang YS, Zhang Y, Wei JF, Guo HX, *Parasitol Res*, 2010, **107**, 873-8
13. Cui L, Su XZ, *Expert Rev Anti Infect Ther*, 2009, **7**, 999-1013
14. You J, Guo H, Mei J, Jiao P, Feng J, Yao M, Xiao S, *Zhongguo Ji Sheng Chong Xue Yu Ji Sheng Chong Bing Za Zhi*, 1994, **12**, 275-8
15. Xiao SH, You JQ, Guo HF, Mei JY, Jiao PY, Yao MY, Zhuang ZN, Feng Z, *Zhongguo Yao Li Xue Bao*, 1999, **20**, 750-4
16. Xiao SH, You JQ, Guo HF, Jiao PY, Mei JY, Yao MY, Feng Z, *Zhongguo Yao Li Xue Bao*, 1998, **19**, 279-81

17. Krishna S, Pulcini S, Fatih F, Staines H, *Trends Parasitol*, 2010, **26**, 517-23
18. Berman PA, Adams PA, *Free Radic Biol Med*, 1997, **22**, 1283-8
19. Xiao SH, You JQ, Gao HF, Mei JY, Jiao PY, Chollet J, Tanner M, Utzinger J, *Exp Parasitol*, 2002, **102**, 38-45
20. Mourao MM, Grunau C, LoVerde PT, Jones MK, Oliveira G, *Parasite Immunol*, 2012, **34**, 151-62
21. Han ZG, Brindley PJ, Wang SY, Chen Z, *Annu Rev Genomics Hum Genet*, 2009, **10**, 211-40
22. Zhao Y, Hanton WK, Lee KH, *J Nat Prod*, 1986, **49**, 139-42
23. Kannan R, Sahal D, Chauhan VS, *Chem Biol*, 2002, **9**, 321-32
24. Abdin AA, Ashour DS, Shoheib ZS, *Biomed Environ Sci*, 2013, **26**, 953-61
25. Messori L, Gabbiani C, Casini A, Siragusa M, Vincieri FF, Bilia AR, *Bioorg Med Chem*, 2006, **14**, 2972-7
26. Semenov A, Olson JE, Rosenthal PJ, *Antimicrob Agents Chemother*, 1998, **42**, 2254-8
27. Klonis N, Crespo-Ortiz MP, Bottova I, Abu-Bakar N, Kenny S, Rosenthal PJ, Tilley L, *Proc Natl Acad Sci U S A*, 2011, **108**, 11405-10
28. Eckstein-Ludwig U, Webb RJ, Van Goethem ID, East JM, Lee AG, Kimura M, O'Neill PM, Bray PG, Ward SA, Krishna S, *Nature*, 2003, **424**, 957-61
29. Forrest GL, Gonzalez B, *Chem Biol Interact*, 2000, **129**, 21-40
30. Pesce ER, Cockburn IL, Goble JL, Stephens LL, Blatch GL, *Infect Disord Drug Targets*, 2010, **10**, 147-57
31. Waldeck-Weiermair M, Jean-Quartier C, Rost R, Khan MJ, Vishnu N, Bondarenko AI, Imamura H, Malli R, Graier WF, *J Biol Chem*, 2011, **286**, 28444-55
32. Tamai S, Iida H, Yokota S, Sayano T, Kiguchiya S, Ishihara N, Hayashi J, Mihara K, Oka T, *J Cell Sci*, 2008, **121**, 2588-600
33. Petris MJ, *Pflugers Arch*, 2004, **447**, 752-5
34. Fedorenko A, Lishko PV, Kirichok Y, *Cell*, 2012, **151**, 400-13
35. Tsuchida T, Zou J, Saitoh T, Kumar H, Abe T, Matsuura Y, Kawai T, Akira S, *Immunity*, 2010, **33**, 765-76
36. Faghiri Z, Skelly PJ, *FASEB J*, 2009, **23**, 2780-9
37. Fu HL, Valiathan RR, Arkwright R, Sohail A, Mihai C, Kumarasiri M, Mahasen KV, Mobashery S, Huang P, Agarwal G, Fridman R, *J Biol Chem*, 2013, **288**, 7430-7
38. Carafoli F, Hohenester E, *Biochim Biophys Acta*, 2013, **1834**, 2187-94
39. Lemeer S, Bluwstein A, Wu Z, Leberfinger J, Muller K, Kramer K, Kuster B, *J Proteomics*, 2012, **75**, 3465-77

40. Koo DH, McFadden C, Huang Y, Abdulhussein R, Friese-Hamim M, Vogel WF, *FEBS Lett*, 2006, **580**, 15-22
41. Osman A, Niles EG, Verjovski-Almeida S, LoVerde PT, *PLoS Pathog*, 2006, **2**, 0536-50
42. Song G, Ouyang G, Bao S, *J Cell Mol Med*, 2005, **9**, 59-71
43. Piiper A, Zeuzem S, *Curr Pharm Des*, 2004, **10**, 3539-45
44. Speidel D, Varoqueaux F, Enk C, Nojiri M, Grishanin RN, Martin TF, Hofmann K, Brose N, Reim K, *J Biol Chem*, 2003, **278**, 52802-9
45. King TD, Gandy JC, Bijur GN, *Exp Cell Res*, 2006, **312**, 3693-700
46. Wang H, Brautigan DL, *J Biol Chem*, 2002, **277**, 49605-12
47. Enkhbayar P, Kamiya M, Osaki M, Matsumoto T, Matsushima N, *Proteins*, 2004, **54**, 394-403
48. Kuss M, Adamopoulou E, Kahle PJ, *J Neurochem*, 2014, **129**, 980-7
49. Paavola KJ, Hall RA, *Mol Pharmacol*, 2012, **82**, 777-83
50. Oldham WM, Hamm HE, *Nat Rev Mol Cell Biol*, 2008, **9**, 60-71
51. DeFea KA, *Cell Signal*, 2011, **23**, 621-9
52. Mukherjee A, Veraksa A, Bauer A, Rosse C, Camonis J, Artavanis-Tsakonas S, *Nat Cell Biol*, 2005, **7**, 1191-201
53. Royet J, Bouwmeester T, Cohen SM, *EMBO J*, 1998, **17**, 7351-60
54. Cormier S, Le Bras S, Souilhol C, Vandormael-Pournin S, Durand B, Babinet C, Baldacci P, Cohen-Tannoudji M, *Mol Cell Biol*, 2006, **26**, 3541-9
55. Lossie AC, Lo CL, Baumgarner KM, Cramer MJ, Garner JP, Justice MJ, *BMC Genet*, 2012, **13**, 106
56. Xiao SH, You JQ, Mei JY, Guo HF, Jiao PY, Sun HL, Yao MY, Feng Z, *Zhongguo Yao Li Xue Bao*, 1997, **18**, 363-7
57. Wisniewski JR, Zougman A, Nagaraj N, Mann M, *Nat Methods*, 2009, **6**, 359-62
58. Griffin TJ, Xie H, Bandhakavi S, Popko J, Mohan A, Carlis JV, Higgins L, *J Proteome Res*, 2007, **6**, 4200-9
59. Sandberg A, Lindell G, Kallstrom BN, Branca RM, Danielsson KG, Dahlberg M, Larson B, Forshed J, Lehtio J, *Mol Cell Proteomics*, 2012, **11**, M112 016998-14
60. Snelling WJ, Lin Q, Moore JE, Millar BC, Tosini F, Pozio E, Dooley JS, Lowery CJ, *Mol Cell Proteomics*, 2007, **6**, 346-55
61. Liu S, Cai P, Hou N, Piao X, Wang H, Hung T, Chen Q, *Mol Biochem Parasitol*, 2012, **182**, 75-82
62. Hong Y, Peng J, Jiang W, Fu Z, Liu J, Shi Y, Li X, Lin J, *Mol Cell Proteomics*, 2011, **10**, M110 006098-11

Figure legends

Fig. 1. Numbers of differentially expressed proteins from *S. japonicum* treated with ART.

(A) Numbers of differentially expressed proteins from *S. japonicum* treated with ART during aging process; (B) The overlap of proteins significantly differentially expressed between each two developmental stages treated with ART; (C) Proteins significantly differentially expressed between each two development stages without treatment; (D) 90 drug related proteins (DRPs) and 156 aging-related proteins (ARPs). DROPs: drug-related-only proteins; ADRPs: aging and drug-related-only proteins.

Fig. 2. Validation of iTRAQ data by qPCR.

(A) qPCR ratios correspond to the relative expression of the target mRNA between the sample ART1, CON2, ART2, CON3, ART3 and the control CON1 (means of three biological replicates, and positive and negative deviations for the respective gene are shown). (B) The fold changes after ART treatment during the *S. japonicum* aging process. The abbreviations and their corresponding protein IDs (Uniprot accession numbers) are presented below. *Txn12* (C1LIE3), Thioredoxin-like 2; *Cbr1* (C1LRC9), Carbonyl reductase 1; *SJCHGC03473* (Q5BXE0), SJCHGC03473 protein; *DSSI* (C1LF72), 26 proteasome complex subunit DSS1; *Ppia* (C1LXK5), Peptidyl-prolyl cis-trans isomerase; *SJCHGC06635* (Q5DGF9), SJCHGC06635 protein; *STH1* (C1L8Z6), Putative Stress-induced-phosphoprotein 1; *eIF4G 3* (C1LD76), Putative eukaryotic translation initiation factor 4 gamma, 3; *OGDC-E2* (C1L595), 2-oxoglutarate dehydrogenase E2 component.

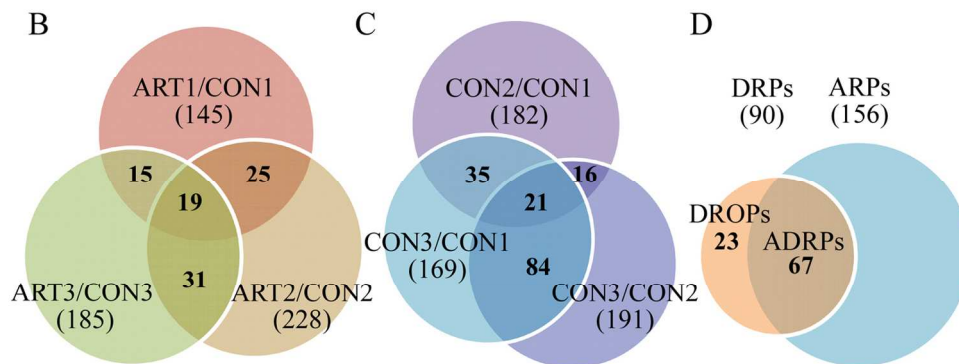
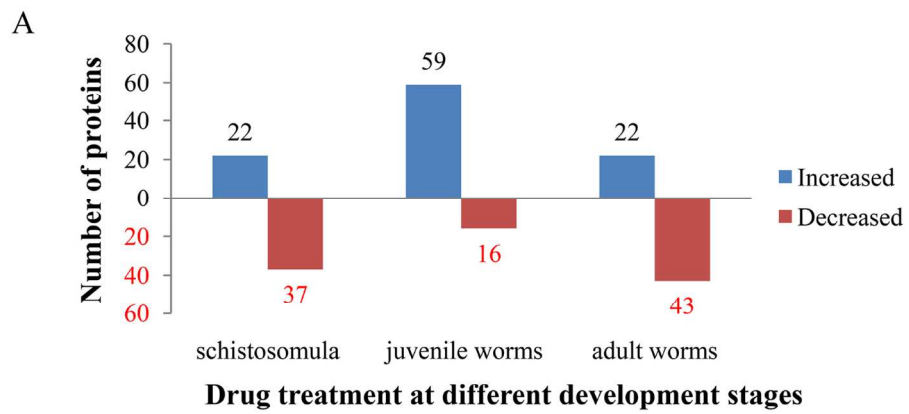
Fig. 3. Functional classifications (A) and localizations (B) of differentially expressed proteins.

Fig. 4. Pathways of ART stress responses in *S. japonicum*.

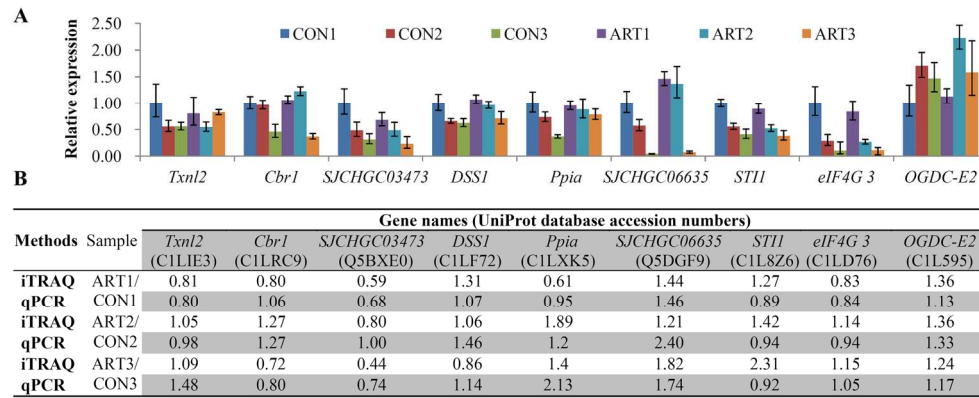
Asterisks indicate DROPs that are involved in glycolysis, TCA cycle, xenobiotics metabolism, exocytosis, notch signal, replication, pre-rRNA processing and protein synthesis. The remaining unmarked proteins are ADRPs, which might be less important in the response to ART. Abbreviations: DROPs, Drug-related-only proteins; ADRPs, aging and drug-related proteins; CAPS, calcium-dependent activator protein for secretion; LRR, leucine-rich repeat containing protein; AQP-3, aquaporin-3; DDR, discoidin domain receptor; Hop1, stress-induced-phosphoprotein 1; PP1, protein phosphatase-1; PPIase, peptidylprolyl isomerase; Nle1, notchless 1; SH3, Sh3 domain containing protein; C1L4V2, uncharacterized protein; CBR1, Carbonyl reductase 1; PKB, protein kinase B; IPP-2, protein phosphatase inhibitor-2; PP1, protein phosphatase 1; GSK3, glycogen synthase kinase-3; OGDHC E2, E2 component of mitochondrial 2-oxoglutarate dehydrogenase complex; LETM1, leucine zipper-EF-hand containing transmembrane protein 1; SPN1, snurportin1; Nubp1, nucleotide-binding protein 1; UPF1, regulator of nonsense transcripts 1; ORC subunit 3, Origin recognition complex subunit 3; NOP56P, nucleolar protein 5A; H2A, histone H2A.

Fig. 5. Pathways enrichment analysis of differentially expressed proteins

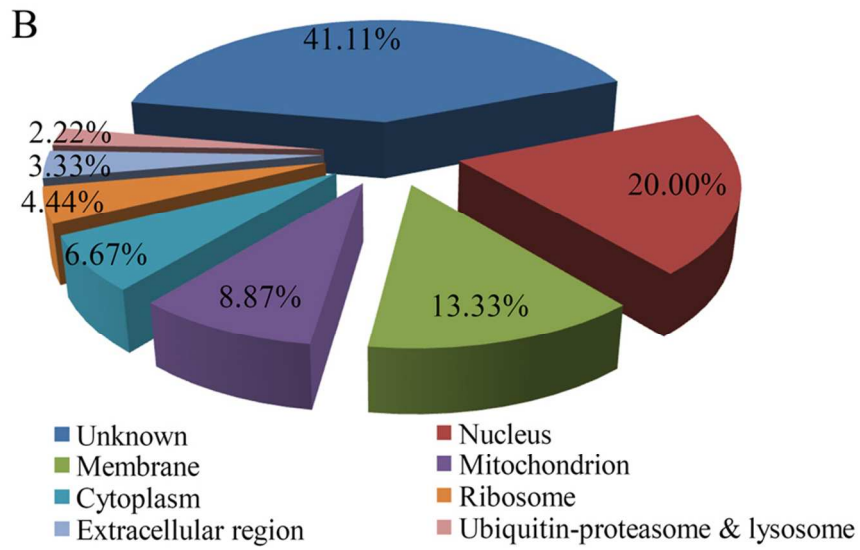
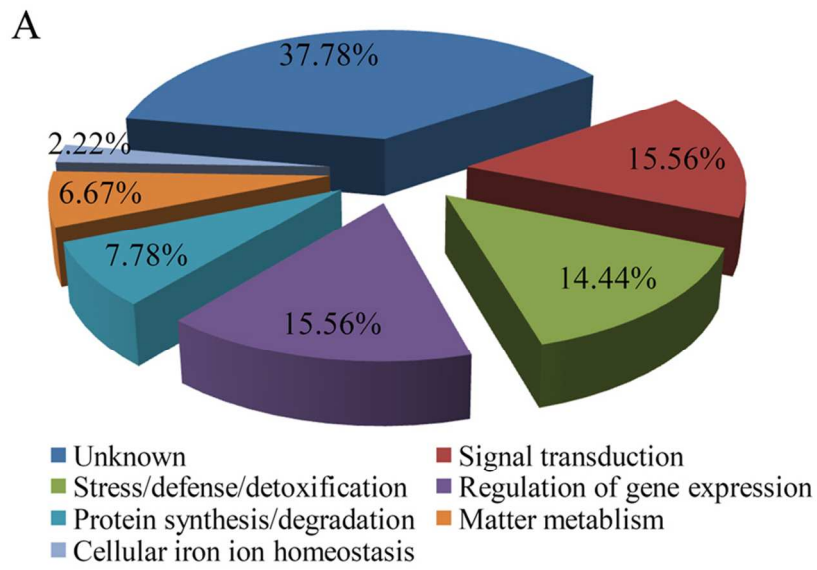
The pathway enrichment statistics was performed by Fisher's Exact Test, and with a corrected p value < 0.05 was considered the most significant pathways.



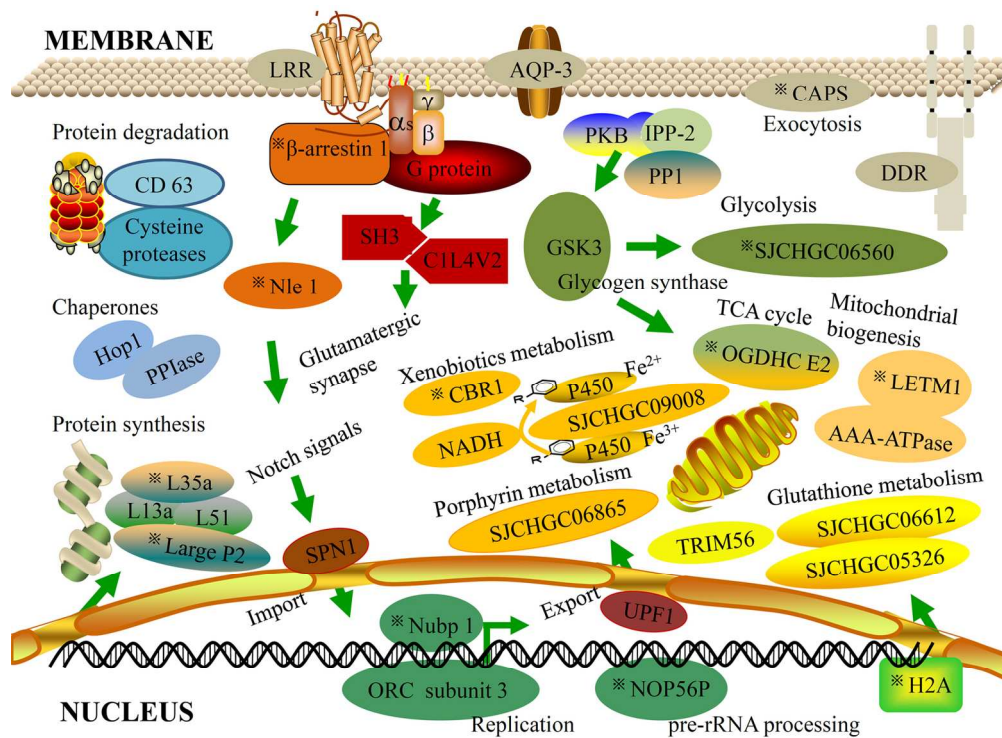
142x118mm (300 x 300 DPI)



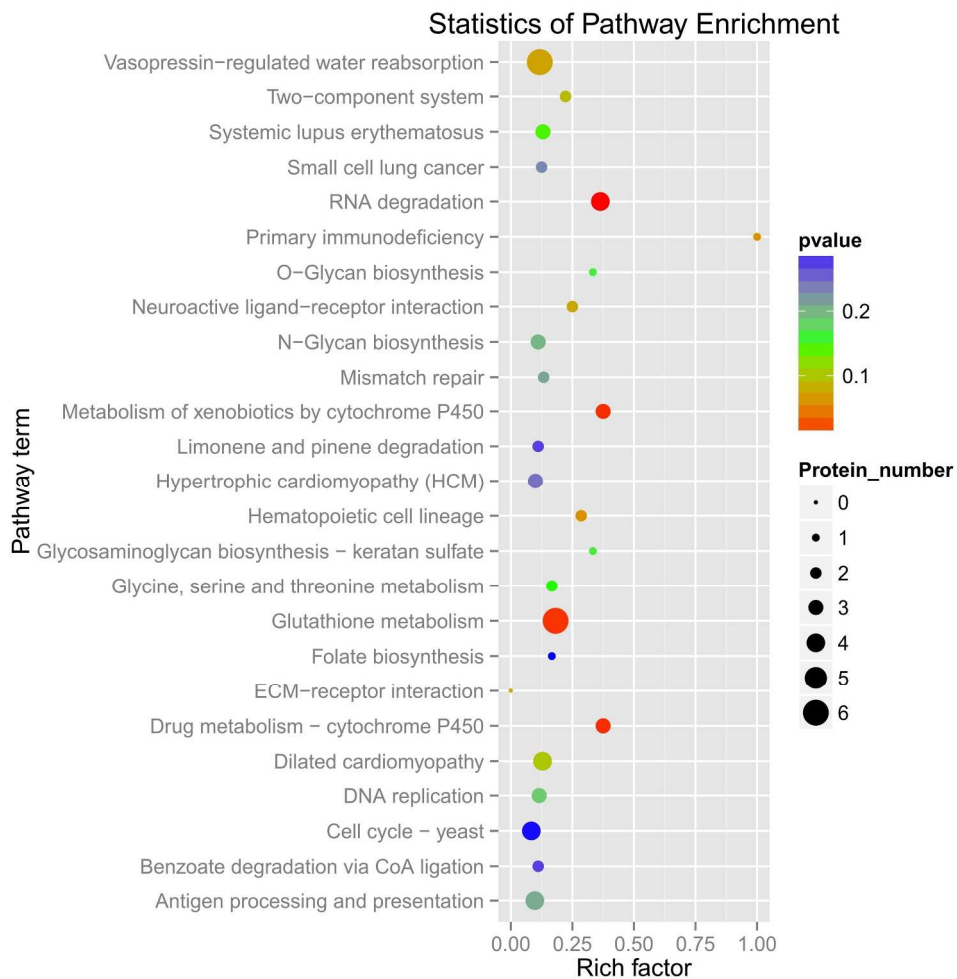
173x70mm (300 x 300 DPI)



82x112mm (300 x 300 DPI)



172x130mm (300 x 300 DPI)



697x694mm (96 x 96 DPI)